

Femtosecond Inscription of the First Order Bragg Gratings in Pure Fused Silica

Mykhaylo Dubov, Vladimir Mezentsev, and Ian Bennion

Photonics Research Group, Aston University,
Aston Triangle, Birmingham, B4 7ET, United Kingdom, m.dubov@aston.ac.uk

ABSTRACT

The fabrication of sub-micron periodic structures beyond diffraction limit is a major motivation for the present paper. We describe the fabrication of the periodic structure of 25 mm long with a pitch size of 260 nm which is less than a third of the wavelength used. This is the smallest reported period of the periodic structure inscribed by direct point-by-point method. A prototype of the add-drop filter, which utilizes such gratings, was demonstrated in one stage fabrication process of femtosecond inscription in the bulk fused silica.

Keywords: femto-second inscription, microfabrication, Bragg gratings

1 INTRODUCTION

Femtosecond microfabrication is one of the enabling technologies for manufacturing of sophisticated 3D photonic devices. Bragg gratings (BG) are ubiquitous components in many composite devices where wavelength selectivity is ultimately required. Manufacturing of the BGs in bulk material is a challenging technological problem involving pinpoint precise fabrication of periodic perturbation of refractive index within or in the vicinity of the waveguide. Femtosecond inscription is a unique technology enabling the fabrication of both the waveguide and the grating in the same set up. The major problem is a submicron pitch size for variation of refractive index required for the First Order BG (FOBG). Thus one has to resort to femtosecond inscription of multiple (2nd -6th) order grating as was recently demonstrated in various fibers [1] including active fibers [2]. Second order gratings were found to be most efficient [1]. However, in vast majority of applications FOBGs with a stop band around 1500 nm are required. It implies a pitch size of 260 nm to provide the required grating period of 535 nm in fused silica.

Sub-micron structures such as voids of similar size have been already demonstrated for tight focusing conditions [3], however the distance between the voids was few microns as opposed to 260 nm needed for BG. This principal requirement of equality of the pitch size and the distance between the peaks along with the waveguide diameter, achievable refractive index contrast, posi-

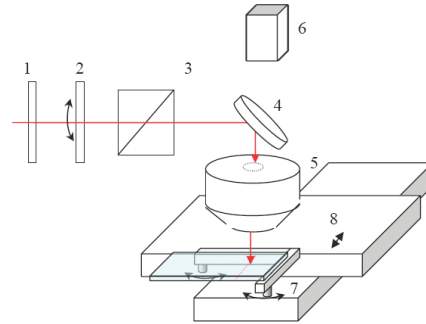


Figure 1: Optical layout for femtosecond inscription. The light passes a shutter (1), a half-wave plate (2), Glan prism (3), and after beamsplitter (4) being focused by a $\times 36$ long working distance microscopic objective (5), and is focused inside the fused silica sample $50 \times 20 \times 1$ mm. The remote CCD camera (6) was used for monitoring and a sample alignment with the help of modified mirror mount (7). This was mount on the manual Z-stage (not shown on the Figure). The translation of the sample in a horizontal plane was done by the 2D computer control stage (8).

tioning depth comprise a set of contradictory constraints leading to usage of moderately tight focusing. The fabrication of sub-micron periodic structures beyond diffraction limit is a major motivation for the present paper.

We describe the fabrication of the periodic structure of 25 mm long with a pitch size of 260 nm. This pitch size is less than a third of the wavelength of the laser light used. This is the smallest period for BG manufactured in the bulk of glass sample.

2 EXPERIMENTAL SETUP

The schematic of the experimental set-up is presented in Figure 1. It is similar to [1], but a fused silica slide was positioned horizontally to exploit the advantages of the 2D patterning in a transverse geometry. Pulse source comprises the laser system (Spectra Physics), the Spitfire amplifier (Positive Light), and Tsunami femtosecond mode-locked generator (Spectra Physics). It is capable to produce 120-150 fs pulses at the wavelength of 796 nm at 1 kHz repetition rate. The computer controlled atten-

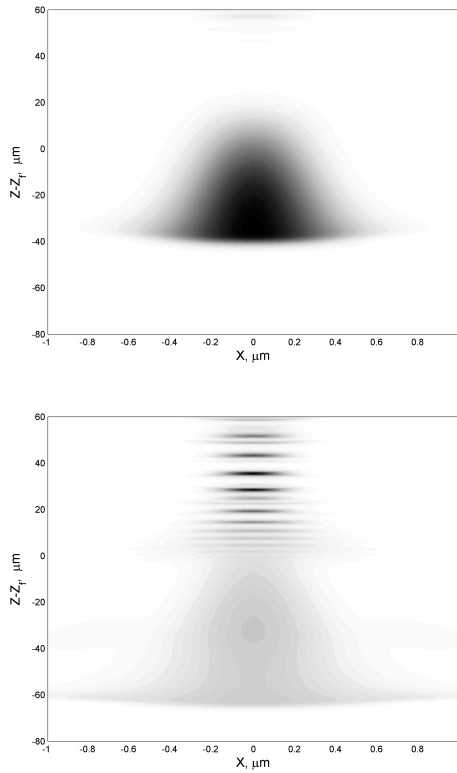


Figure 2: Density plots of the residual plasma concentration for different initial pulse energies: top – Subcritical, 68 nJ; bottom – Supercritical, 187 nJ;

uation is realized with the half wave-plate (2) mounted on the motorized rotational stage, and a Glan prism (3). Electronic shutter (1) is installed immediately after the laser system output window. He-Ne laser (not shown in the Figure) is used for alignment.

The femtosecond inscription of all structures was performed after careful positioning of the sample surface at the same distance from the objective on both ends of the scanning range with the help of a modified mirror mount. We have used $\times 36$ NA=0.5 long working distance (Schwarzschild) reflecting objective to focus the laser radiation. This objective has a variable correction ring (to correct a spherical aberration of a sharply focused beam) for the sample thickness - focusing depth - up to 1 mm. The optimal correction was found as a result of multiple thorough experiments for smallest period of the grating. The remote CCD-camera (6) was used for alignment and on-line monitoring of the inscription process. The z-axis stage (not shown on the Figure) was mounted on top of the top (Y) stage. For grating fabrication we used mainly scanning in Y-direction, as this provides for a triple reduction of the errors in positioning (< 50 nm) as compared with the motion along the X (bottom axis). The objective has an obscuration about 15%, and a working distance of 8.6 mm. For in-

scription of the 535 nm period the stage was moved with a speed of 0.535 mm/sec while the laser had a 1kHz repetition rate. Typical pulse energy for grating fabrication was 600 nJ.

3 NUMERICAL MODELING

We have found that generally, the larger is the pulse energy the smaller spatial structures can be inscribed provided that the material damage threshold is not exceeded. We have performed numerical modeling to determine qualitative features of the inscription process for supercritical regimes when the pulse power exceeds a self-focusing threshold.

For the purposes of this paper, a simplified physical model is used, essentially similar to that described by Feng et al. [4]:

$$i\mathcal{E}_z + \frac{1}{2k}\Delta_{\perp}\mathcal{E} + k_0n_2|\mathcal{E}|^2\mathcal{E} = \frac{k''}{2}\frac{\partial^2\mathcal{E}}{\partial t^2} - \frac{i\sigma}{2}(1+i\omega\tau)\rho\mathcal{E} - i\frac{\beta^{(K)}}{2}|\mathcal{E}|^{2(K-1)}\mathcal{E} \quad (1)$$

$$\frac{\partial\rho}{\partial t} = \frac{1}{n_b^2}\frac{\sigma_{bs}}{E_g}\rho|\mathcal{E}|^2 + \frac{\beta^{(K)}}{K\hbar\omega}|\mathcal{E}|^{2K} \quad (2)$$

The terms on the left-hand side of Eq.(1) describe effects of beam diffraction, group velocity dispersion (GVD), and Kerr nonlinearity. The latter is responsible for a catastrophic self-focusing which is limited by the effects described by terms on the right-hand side of Eq.(1), namely, dispersion, plasma absorption and defocusing, and multi-photon absorption. In Eq.(1) the laser beam propagation along the z axis is assumed and this equation is essentially a reduced paraxial approximation of the wave equation for the complex electric field envelope \mathcal{E} with a carrier frequency ω in the moving frame of coordinates. Here $k = n_b k_0 = n_b \omega / c$ is the propagation vector, $k'' = \partial^2 k(\omega) / \partial \omega^2$ is the GVD parameter, $n_b(\omega)$ is a linear refractive index of the bulk medium, n_2 is the nonlinear coefficient describing nonlinear self-modulation (Kerr effect) such that $n_2|\mathcal{E}|^2$ is a nonlinear contribution to the refractive index, σ_{bs} is the cross section for inverse Bremsstrahlung, τ is the electron relaxation time, E_g is the ionization energy, and the quantity $\beta^{(K)}$ controls the K -photon absorption. Equation (2) implements the Drude model for electron-hole plasma in the bulk of silica and describes the evolution of the electron density ρ . The first term on the right-hand side is responsible for the avalanche impact ionization and the second term — for the ionization resulting from MPA. Equation (2) is suitable for description of the sub-picosecond laser pulses when plasma diffusion is negligible.

For the fixed pulsewidth used in simulations, the critical energy of 116 nJ corresponds to a critical power $P_{cr} = \lambda_0^2 / 2\pi n_b n_2 \approx 2.3$ MW required for self-focusing

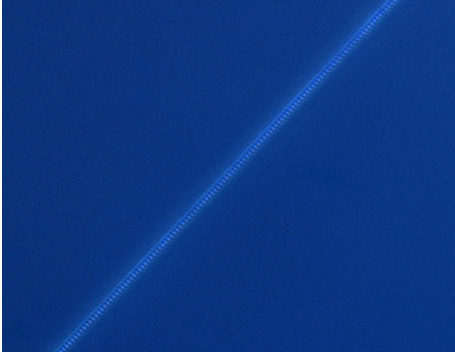


Figure 3: Grating with a pitch size 260 nm (period 535 nm)

in fused silica with $n_b = 1.453$ being the linear refraction index and $n_2 = 3.2 \times 10^{-16} \text{ cm}^2/\text{W}$ the nonlinear refraction index. Critical power is proven to be a crucial parameter to determine the evolution of the collapsing beam. We assume the laser wavelength λ_0 to be 800 nm and the focusing lens to have $f = 40 \text{ mm}$. The other parameters for fused silica, used in simulations are GVD coefficient $k'' = 361 \text{ fs}^2/\text{cm}$, inverse Bremsstrahlung cross section $\sigma_{bs} = 2.78 \times 10^{-18} \text{ cm}^2$. Multiphoton absorption coefficient can be expressed as $\beta^{(K)} = \hbar\omega\sigma_K\rho_{at}$, with $\rho_{at} = 2.1 \times 10^{22} \text{ atoms/cm}^3$ being a material concentration and $\sigma_K = 1.3 \times 10^{-55} \text{ cm}^2/\text{W}^K/\text{s}$. Five-photon ionization with $K = 5$ and $E_g = 7.6 \text{ eV}$ is assumed in fused silica.

The Equation (2) defines an important threshold for the light intensity $I_{MPA} = (K\hbar\omega\rho_{BD}/t_p\beta^{(K)})^{1/K}$ when the multi-photon ionization becomes a dominant mechanism. The plasma breakdown density $\rho_{BD} = 1.7 \times 10^{21}$ is another physical threshold. Being important physical thresholds, both I_{MPA} and ρ_{BD} were used in numerical characterization of the inscription process to determine an inscription domain in parameter space. A condition $I > I_{MPA}$ was usually chosen to determine an inscription threshold and a condition $\rho < \rho_{BD}$ — to determine a the threshold of the material damage .

Figure (2) shows a set of results for asymptotic distribution of plasma density when electromagnetic field is vanished. It illustrates our major finding that for supercritical energies plasma distribution becomes finely patterned (Fig. (2, bottom)) as opposed to broadly smooth distribution in subcritical case Fig. (2, top). Fine plasma filaments resulting from the supercritical self-focusing may have spatial diameter 150–200 nm which enables inscription of sub-wavelength structures described in the next section.

4 RESULTS

The experimental setup described above was used to inscribe periodic structures and waveguides. Figure 3

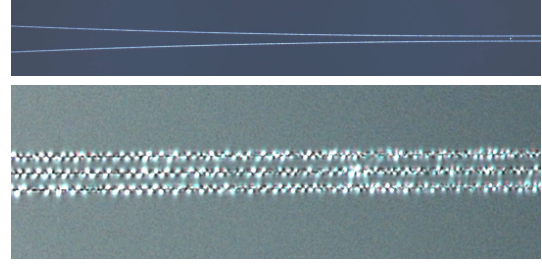


Figure 4: Typical coupler inscribed with the tight focusing setup (top). Stresses are visualized in cross-polarized light (bottom).

shows the grating with the period of 535 nm formed with the pitches of modified refractive index with a diameter of about 150–200 nm. Such a period corresponds to FOBG for $\lambda = 1550 \text{ nm}$. The microscopic DIC image of such grating was produced using a $\times 63$ plan-Neofluar objective (NA=0.8). Visual inspection of the gratings was performed along the whole 26 mm long sample. It was found to be as good as the second order Bragg gratings inscribed in fibre by similar point-by-point method [1]. We have tried to put a FOBG between the two parallel (middle) arms of the symmetrical 2×2 coupler (Fig. 4, top)). Smooth waveguides were inscribed at the speed of 0.01 mm/s with the same set-up. Fig.4 (top) shows a microscopic images of such grating assisted 2×2 coupler. The grating was manufactured prior the coupler fabrication. White dot near the right edge of the picture marks the position of the grating. We characterize the distribution of the refractive index with the commercial QPM software by IATIA [5]. This method enables the cumulative phase measured along the propagation axis. To calculate the refractive index contrast the information about depth of the structure is required. The visual contrast of the FOBG was of the same order as in a smooth waveguide. We found that the index contrast induced by femtosecond laser was less or around 5×10^{-4} . It is certainly enough to produce high quality gratings, however, the microscopic waveguides with such a low refractive index contrast become weakly guiding [6]. The latter factor is a serious fundamental constraint for designing couplers and other photonic devices because it leads to high bending losses. There are two principal ways to increase the strength of the waveguide, either have larger index contrast, or increase the cross-section of the track. This second approach is usually combined with an astigmatic beam shaping either by optical slit [7] or by the cylindrical telescope [8]. We suggest another approach — to draw multiple tracks close each other thus forming a bundled “superwaveguide” with a much larger effective cross-section. The simulations reveal that this method is very flexible, simple, and energy efficient. However neither multiple parallel inscription nor repetitive in-

scription in attempt to increase the contrast over the same track was unsuccessful due to significant residual stresses. The microscopic investigation in crossed polarized light (Fig. 4, bottom) reveals residual stresses in a surrounding material. Figure (4, bottom) shows few tracks produced by multiple repetitive scans. Every successive scan made the stresses even more pronounced. This seems to be a feature of both the low repetition rate femtosecond inscription with sharp focusing and a fused silica as a target material [9].

In a second series of experiments, off-axis parabolic mirror (effective $NA=0.08$, $f = 25$ mm) was used to provide loose coupling for inscription of the waveguides. The simulations described in previous section emphasize the importance of the nonlinear effects like self-focusing and beam filamentation. Proper choice of the inscription power and depth enables production of both multiple scans over the same track (up to ten times) and bundles of the waveguides with practically arbitrary separation. The individual cores have the same index contrast and the dimensions around 6×30 microns due to limitations of loose focusing. The tracks presented on the Fig. 5 demonstrate easy coupling and much lower losses compared to waveguides manufactured with sharply focusing objectives. The near-field mode of such bundled waveguide comprising three cores is shown in inset. Top track (double core with single scan each) was the strongest. The middle track had two successive scans. The bottom track was the weakest one, having only a single scan. It is worth to mention, that the nonlinear method has much wider inscription window (500%) than sharp focusing one (20%). Thus, we conclude that combination of methods is found to inscribe various photonics components for hybrid photonic devices such as grating assisted couplers and many others. The flexibility of the described methods also enables the engineering of the optimal profile of the index along the bends to further reduce bending losses.

5 CONCLUSION

We have fabricated a first order Bragg Grating in bulk fused silica with a pitch size of 260 nm which is less than a third of the wavelength used. This is the smallest reported period of the periodic structure inscribed by direct point-by-point method. It was numerically found that such small structures result from fine plasma filaments produced during supercritical self-focusing. Prototype components of the grating assisted add-drop filter have been experimentally demonstrated. FOBG was manufactured in one stage fabrication process of femtosecond inscription in the bulk fused silica. Bundled waveguides are demonstrated to facilitate stronger waveguiding with reduced bending losses.

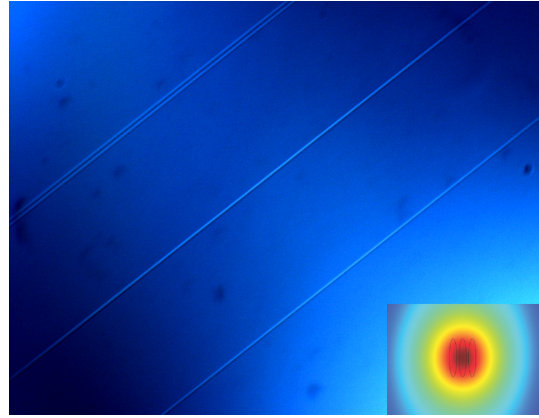


Figure 5: The nonlinear regime of femtosecond inscription produces smooth tracks with the possibility of multiple successive scans and multiple collinear tracks. The separations between waveguides are 100 micrometers. Upper (double) track consist of two single ones, middle waveguide obtained by two successive scans one on top another, and single scan was done for the bottom one.

REFERENCES

- [1] A. Martinez, M. Dubov, I. Khrushchev, and I. Bennion, "Direct writing of fibre Bragg gratings by femtosecond laser", *Electron.Lett.* **40** (19),1170, 2004.
- [2] Yicheng Lai et al, "Er:Yb Fiber Grating Laser Based on Femtosecond Laser Inscription Technique", BGPP-2005.
- [3] Wang Dan-Ling et al, "Sub-diffraction-Limit Voids in Bulk Quartz Induced by Femtosecond Laser Pulses", *Chinese Phys. Lett.*, **18**, 65, 2001.
- [4] Q. Feng, et al, "Theory and simulation on the threshold of water breakdown induced by focused ultrashort laser pulses," *IEEE Journal of Quantum Electronics*, **33**, 127, 1997.
- [5] Quantative Phase Microscopy (QPM) <http://www.iatia.com.au/products/qpm.asp>
- [6] M.Dubov, V.Mezentsev, I.Bennion, "Method for Characterisation of Weakly Guiding Waveguides by Measuring Mode Field Diameter, CJ-1290, CLEO-Europe-2005.
- [7] M. Ams, et al., "Slit beam shaping method for femtosecond laser direct-write fabrication of symmetric waveguides in bulk glasses", *Opt. Express*, **13**, 5676, 2005.
- [8] R. Osellame, et al., "Femtosecond writing of active optical waveguides with astigmatically shaped beams", *J. Opt. Soc. Am. B* **20**, 1559, 2003.
- [9] S.M. Eaton, et al., "Heat accumulation effects in femtosecond laser written waveguides with variable repetition rate", *Opt. Express* **13**, 4708, 2005.